Added Value of Baseline ^{18}F-FDG Uptake in Serial ^{18}F-FDG PET for Evaluation of Response of Solid Extracerebral Tumors to Systemic Cytotoxic Neoadjuvant Treatment: A Meta-Analysis

Henriëtte M.E. Quarles van Ufford[1], Harm van Tinteren[2], Sigrid G. Stroobants[3], Ingrid I. Riphagen[4], and Otto S. Hoekstra[5]

[1]Department of Radiology and Nuclear Medicine, University Medical Center Utrecht, Utrecht, The Netherlands; [2]Comprehensive Cancer Center and Netherlands Cancer Institute, Amsterdam, The Netherlands; [3]Department of Nuclear Medicine, University Antwerpen, Antwerp, Belgium; [4]Faculty of Medicine, Unit for Applied Clinical Research, University of Science and Technology, Trondheim, Norway; and [5]Department of Nuclear Medicine and PET Research, VU University Medical Center, Amsterdam, The Netherlands

The purpose of this study was to test the hypothesis that the level of baseline ^{18}F-FDG uptake in the primary tumor adds value to its relative change in ^{18}F-FDG uptake in serial PET scans in predicting the histopathologic response to systemic cytotoxic neoadjuvant treatment of patients with solid extracerebral tumors. **Methods:** We performed a literature search from January 1995 through November 2008 using PubMed and Embase. Two reviewers independently selected eligible studies for possible inclusion in the meta-analysis by reviewing titles and abstracts. Inclusion criteria were at least 10 patients, ^{18}F-FDG PET before and after therapy, ^{18}F-FDG PET performed with the intention of monitoring the response of solid extracerebral tumors in humans to cytotoxic neoadjuvant systemic therapy, attenuation-corrected ^{18}F-FDG PET studies, and studies presenting individual patient data (PET results and histopathologic reference test after treatment). Multilevel logistic regression was used to assess the effect of relative change of ^{18}F-FDG uptake ([baseline – end]/baseline) and baseline ^{18}F-FDG uptake value with type of tumor and type of treatment as level 1 covariates. **Results:** Nineteen studies (all observational; a total of 438 patients [median, 23 patients per study; range, 10–40]) were included, aiming at the accuracy of PET versus histopathology. To quantify PET, maximum standardized uptake value (SUV) was used in 6 studies, mean SUV in 7, SUV (subtype unclear) in 1, tumor-to-background ratio in 3, and dose uptake ratio in 1. The average overall histopathologic response rate was 0.47 (median, 0.50), ranging from 0.17 to 0.88. The relative change in ^{18}F-FDG uptake was the strongest indicator ($P < 0.0001$) for tumor response. Baseline ^{18}F-FDG was not significantly associated as a main factor; however, a significant interaction of baseline uptake and relative change after therapy was observed ($P < 0.001$). **Conclusion:** Relative change in ^{18}F-FDG uptake was the strongest indicator for tumor response, but the level of baseline ^{18}F-FDG uptake in the primary tumor provided additional information about prediction of response to therapy. These data corroborate and extend the need for standardization, quality assurance, and control of PET studies quantifying ^{18}F-FDG in oncologic treatment monitoring.

Key Words: ^{18}F-FDG PET; response evaluation; serial PET

J Nucl Med 2010; 51:1507–1516
DOI: 10.2967/jnumed.110.075457

During the last decade, ^{18}F-FDG PET has become important for the diagnosis, staging, prognosis, and evaluation of treatment response in oncology (*1*). In the neoadjuvant setting, ^{18}F-FDG PET examinations before, during, or after therapy have been investigated to evaluate and monitor therapy response, predict prognosis, and guide decisions on postsurgical treatment. The need for quantitative assessment of metabolic response increases, and it is expected that PET will be incorporated in the response evaluation criteria of solid tumors.

In the context of response evaluation, most studies focus on the relative change of ^{18}F-FDG uptake as an index for metabolic response. Additionally, the level of baseline ^{18}F-FDG uptake may have prognostic value (*2*). Relative change does not account for this potential effect modifier. The aim of this meta-analysis was to qualitatively test the hypothesis that the level of baseline ^{18}F-FDG uptake in the primary tumor has added value to relative change in ^{18}F-FDG uptake in serial PET scans in evaluating response to systemic cytotoxic neoadjuvant treatment of patients with solid extracerebral tumors.

MATERIALS AND METHODS

Literature Search

A formal computer-assisted search was performed in the medical databases PubMed (Medline included) and Embase from January 1995 through November 2008. Both text words and medical subject headings were used. The full-search algorithm can be obtained in Supplemental Table 1 (supplemental materials are available online only at http://jnm.snmjournals.org). In addition, a

Received Jan. 27, 2010; revision accepted Jul. 14, 2010.
For correspondence or reprints contact: Henriëtte M.E. Quarles van Ufford, Department of Radiology, University Medical Center Utrecht, HP E.01.132, Heidelberglaan 100, 3584 CX, Utrecht, The Netherlands.
E-mail: h.m.e.quarlesvanufford@umcutrecht.nl

TABLE 1. Patient Characteristics of 19 Studies Reviewed

Study	Design	Total no. of patients in analysis	Age (y)		Sex*	No. of lesions or patients included in meta-analysis	Tumor type	Neoadjuvant therapy	
			Mean	Range				Type	Amount of cycles
Schulte et al. (*5*)	Prospective	27	17	5–36	17	27	Osteogenic sarcoma	Chemotherapy	
Franzius et al. (*6*)	Retrospective	17	13	5–36	13	17	Osteosarcoma (n = 11) Ewing's sarcoma (n = 6)	Chemotherapy Chemoradiotherapy in 5 cases of Ewing's sarcoma	4–6
Smith et al. (*7*)	Prospective	30	49	31–72	0	31	Breast cancer	Chemotherapy	8
Nair et al. (*8*)	Unclear	16	17	15–29	8	15	Osteosarcoma	Chemotherapy	3
Brücher et al. (*9*)	Prospective	27	52.9 (±6.1)	37.8–61	23	24	Esophageal squamous cell carcinoma	Chemoradiotherapy	12 continuous days
Ryu et al. (*10*)	Prospective	26	62	47–73	15	26	Non–small cell lung cancer	Chemoradiotherapy	2
Kitagawa et al. (*11*)	Prospective	23	63.8	47–85	18	23	Head and neck carcinoma	Chemoradiotherapy	2
Brink et al. (*12*)	Prospective	20	53.7 (±9.5)	Not mentioned	17	20	Esophageal carcinoma	Chemoradiotherapy	4
Chen et al. (*13*)	Retrospective	15	44	32–56	0	16	Locally advanced breast cancer	Chemotherapy	Unclear
Wieder et al. (*14*)	Unclear, consecutive	38	60 (±6.8)	Not mentioned	27	29	Esophageal squamous cell carcinoma	Chemoradiotherapy	28 d
Song et al. (*15*)	Prospective	74	63	45–74	29	32	Locally advanced esophageal cancer	Chemoradiotherapy	3
Cascini et al. (*16*)	Prospective	33	58	29–74	20	33	Locally advanced rectal cancer	Chemoradiotherapy	3
Huang et al. (*17*)	Prospective	10	19	4–47	8	10	Primary osteosarcoma	Chemotherapy	Not mentioned
Wieder et al. (*18*)	Unclear	24	60	33–71	20	24	Adenocarcinoma of the esophagogastric junction	Chemotherapy	2
Iagaru et al. (*19*)	Retrospective	14	36 (±14)	18–56	8	14	Bone and soft-tissue sarcomas	Chemotherapy	Not mentioned
Nishiyama et al. (*20*)	Retrospective	21	54.5	29–80	0	21	Advanced gynecologic cancer	Chemotherapy Chemoradiotherapy	3–6 4
Benz et al. (*21*)	Prospective	20	49	32–66	10	20	Soft-tissue sarcomas	Chemotherapy (not mentioned) Chemoradiotherapy	 14
Smithers et al. (*22*)	Prospective	45	Not mentioned		Not mentioned	40	Adenocarcinoma of the esophagus	Chemotherapy Chemoradiotherapy	2 2
Ye et al. (*23*)	Prospective	15	17	7–31	15	15	Osteogenic sarcoma	Chemotherapy	2

*Amount of male patients.
Data in parentheses are SD.

TABLE 2. Definition of Response Differs According to Tumor Type: Histopathologic Evaluation System

Tumor type	Evaluation system	Definition of response
Esophageal carcinomas	Mandard system (*24*)	No or only a few scattered residual tumor cells (regression scores 1 and 2)
Bone tumors	Salzer–Kuntschik system (*25*)	Salzer–Kuntschik grades I–III: less than 10% residual vital tumor area (grade I, 0%; II, single vital areas; and III, <10%)
Breast cancer (*7*)	Previously described criteria (*26,27*)	Macroscopic (absence of macroscopically visible tumor) or microscopic (histologic absence of invasive tumor cells) response
Breast cancer (*13*)	—	No recognizable invasive tumor cells (ductal carcinoma in situ may be present)
Head and neck cancer (*11*)	—	No viable residual tumor cells in any section
Non–small cell lung cancer	—	Tissue negative for malignant cells
Locally advanced rectal cancer	—	Complete regression or rare residual cancer cells
Gynecologic cancer	—	No tumor (complete response) or residual microscopic disease only

manual cross-reference search of eligible and review papers was performed to identify additional possible articles.

Study Selection

Three reviewers independently selected studies for possible inclusion in the meta-analysis by reviewing titles and abstracts. Differences were resolved by consensus. To be eligible for the meta-analysis, a study had to fulfill the following inclusion criteria: at least 10 patients, ^{18}F-FDG PET before and after therapy, ^{18}F-FDG PET performed with the intention of monitoring the response of solid extracerebral tumors in humans to cytotoxic neoadjuvant systemic therapy, attenuation-corrected ^{18}F-FDG PET studies, and studies presenting individual patient data (PET results and histopathologic reference test after treatment). Duplicate studies on the same patients, studies using only γ-camera coincidence imaging, studies written in a language other than English or German, and reviews and abstracts were excluded. The last 2 categories were used for cross-referencing. No unpublished data or data from abstracts were used.

Data Abstraction and Quality Assessment

Two reviewers independently extracted the following items from the studies: study design (prospective, retrospective but consecutive, retrospective inclusion), patient characteristics, PET characteristics (qualitative and quantitative), and reference test or histopathologic evaluation system.

We considered the description of PET as adequate if the publication reported details on the scanner type, the timing of scanning after injection, a clear description of quantitative procedures including region-of-interest (ROI) methodology, and the performance of attenuation correction.

Statistical Analysis

Dichotomized histopathologic response (response or no response) was the primary endpoint. Individual patient data consisted of baseline and relative change of ^{18}F-FDG uptake. Baseline PET data were missing for 6 individuals (1%) in different studies and missing for the second PET measurement for 38 individuals (8.7%). For overall consistency, these missing values were imputed by regression (*3*).

Multilevel logistic regression was used to assess the effect of relative change of ^{18}F-FDG uptake ([baseline – end]/baseline), baseline ^{18}F-FDG uptake value, type of tumor (sarcoma, esophageal carcinoma, or other), type of treatment (chemotherapy or chemoradiotherapy), and type of measurement (standardized uptake value [SUV], tumor-to-background ratio, or dose uptake ratio) as level 1 covariates. All sarcomas were treated exclusively by chemoradiotherapy, and they served as the reference group. Studies were included as random factors (level 2), allowing for random intercepts and random slopes for the differences in relative decrease at level 2. Level 1 factors and interactions were investigated by a backward stepwise procedure in which nonsignificant interactions were excluded in order of largest P value (exclusion at $P > 0.05$).

To quantify the heterogeneity between studies, the median odds ratio (MOR) was calculated (*4*). The MOR quantifies the variation between studies (the second-level variation) by comparing 2 persons from 2 randomly chosen, different studies. The MOR is always greater than or equal to 1. If there is considerable between-study variation, the MOR will be large (the measure is comparable with fixed-effects odds ratio). To quantify the effect of study-level covariates (therapy, tumor type), interval odds ratios were calculated. If the interval contained 1, the (fixed) effect of the study-level variable was large in comparison with the unexplained between-study variation (*4*).

RESULTS

Study Characteristics

Our initial search identified 1,749 studies: the PubMed search identified 917 and the EMBASE search (after exclusion of duplicates) 832 studies. On the basis of title and abstract, 1,632 studies did not meet the inclusion criteria. After reviewing the full text of the remaining 117 studies, we included 19 studies (*5–23*). All were observational studies, aiming at the accuracy of PET versus histopathology. The detailed process by which the articles were selected can be found in the Supplemental Appendix 1.

The 19 studies included data on 438 patients, with a median of 23 patients per study (range, 10–40). Of these

TABLE 3. ^{18}F-FDG PET Characteristics in 19 Studies Reviewed

Study	Scanner	Scan mode	^{18}F-FDG dose (MBq)	Interval between ^{18}F-FDG injection and PET (min)	Interval between end induction therapy and posttreatment PET (d)	Interval between posttreatment PET and surgery (d)	Image reconstruction
Schulte et al. (*5*)	ECAT 931-08-12	Partial	120–300	45–60	12–18	Not mentioned	Multiplicative iterative (*29*)
Franzius et al. (*6*)	ECAT EXACT 921/47	Whole body	3.7/kg	60	Not mentioned	3–28 (mean, 21)	Filtered backprojection, Hanning filter, cutoff at Nyquist frequency
Smith et al. (*7*)	ECAT EXACT 31	Partial	185	0–60*, 60–70	Not mentioned	Not mentioned	Filtered backprojection, Hanning filter, cutoff at Nyquist frequency
Nair et al. (*8*)	ECAT EXACT 47	Whole body	370	45	14	Few days	Whole-body format, Hanning filter, cutoff at cutoff frequency = 0.35 of Nyquist frequency
Brücher et al. (*9*)	ECAT 951/R ECAT EXACT†	Partial	250–270	40	21	<7	Filtered backprojection, Hanning filter, cutoff at 0.4 cycles/pixel
Ryu et al. (*10*)	Scanditronix	Partial	370	45	14	Not mentioned	Filtered backprojection to in-plane resolution of 7 mm in full width at half maximum
Kitagawa et al. (*11*)	Advance	Partial	244–488	40	>28	Not mentioned	Not mentioned
Brink et al. (*12*)	ECAT EXACT 922 (+)	Whole body	5/kg	90	Not mentioned	Not mentioned	Iterative, ordered-subset expectation maximization, segmented attenuation correction
Chen et al. (*13*)	Advance	Partial	259–407	60	Not mentioned	Not mentioned	Corrections of data for random and scattered coincidences and attenuation; Hanning filter
Wieder et al. (*14*)	ECAT EXACT	Partial	300–400	60	21–28	< 7	Iterative, ordered-subset expectation maximization (8 iterations, 4 subsets), postreconstruction smoothing with 4-mm Gaussian filter
Song et al. (*15*)	ECAT HR+ 2D	Whole body	555	60	21–28	Just before	Not mentioned
Cascini et al. (*16*)	ECAT EXACT 47	Whole body	300–385	60	Not mentioned	Few days	Iterative, ordered-subset expectation maximization (2 iterations, 16 subsets)

TABLE 3. (Continued)

Study	Scanner	Scan mode	^{18}F-FDG dose (MBq)	Interval between ^{18}F-FDG injection and PET (min)	Interval between end induction therapy and posttreatment PET (d)	Interval between posttreatment PET and surgery (d)	Image reconstruction
Huang et al. (*17*)	ECAT EXACT	Partial	259–370	45	7	Not mentioned	Not mentioned
Wieder et al. (*18*)	ECAT EXACT	Partial	300–400	40	21–28	21–28	Iterative, ordered-subset expectation maximization (8 iterations, 4 subsets), and then smoothed in 3 dimensions using 4-mm Gaussian filter
Iagaru et al. (*19*)	ECAT EXACT 953A Biograph LSO PET/CT‡	Whole body	550	45 60	7–36 (mean ± SD, 16 ± 9)	Not mentioned	Not mentioned
Nishiyama et al. (*20*)	ECAT EXACT HR+	Whole body	185–200	60	12 (range, 2–24)	Not mentioned (32 [range, 19–40] between chemotherapy and surgery)	Iterative, ordered-subset expectation maximization (2 iterations, 8 subsets)
Benz et al. (*21*)	Biograph Duo	Whole body	7.77/kg	77 ± 8.7	Not mentioned	Not mentioned	Iterative, ordered-subset expectation maximization (2 iterations, 8 subsets), postreconstruction gaussian filter; final image resolution of 8.8 mm in full width at half maximum
Smithers et al. (*22*)	Philips Allegro GSO	Whole body	210–427	45	24–32	Chemotherapy, 4 Chemoradiotherapy, 4.5	Iterative, 3-dimensional row-action maximum-likelihood algorithm
Ye et al. (*23*)	SHR-22000	Partial	370	60	4–14 (median, 8)	2–22 (median, 12)	Hanning filter, cutoff at Nyquist frequency

*Dynamic scan protocol, followed by static emission.
†No information on which scanner individual patients were scanned.
‡Each patient baseline and repeated PET scan obtained on same scanner.

TABLE 4. PET Data Analysis Characteristics of 19 Studies Reviewed

Study	Parameter variable	ROI technique	Observer
Schulte et al. (*5*)	TBR	ROIs were individually defined, expressing maximum tumor uptake, excluding areas of lower uptake within tumor. Identical configuration at contralateral extremity was used to obtain TBR. In each case ROIs > 2.6 cm^2.	2, independent (blinded)
Franzius et al. (*6*)	T/NT	Rectangular ROI was positioned around tumor activity in coronary slice with maximum tumor activity, with boundaries of ROI located just within apparent hypermetabolic zone.	2, in consensus (blinded)
Smith et al. (*7*)	Influx constant K, DUR_{BSA}	ROIs were manually drawn around each lesion. Maximum pixel value of DUR or influx constant K within ROI was recorded.	2, in consensus (blinded)
Nair et al. (*8*)	TBR	Identical ROIs were placed over tumor and contralateral normal limb.	3, independent (not mentioned whether blinded)
Brücher et al. (*9*)	SUV_{mean}	Circular ROI (1.5 cm in diameter) was manually placed in slice with maximum ^{18}F-FDG uptake. SUVs were calculated using average activity values in ROI.	Not mentioned
Ryu et al. (*10*)	SUV_{mean}	SUV of primary tumor was determined as mean value in 12-mm ROI positioned over area with highest activity within tumor as determined by visual analysis.	2, independent (blinded)
Kitagawa et al. (*11*)	SUV_{mean}	Round ROIs (5 mm in diameter) were placed over area of highest ^{18}F-FDG uptake in tumor on static images. SUV = tissue radioactivity concentration (Bq/mL)/injected dose (Bq) per body weight (g).	3, independent (blinded)
Brink et al. (*12*)	SUV_{mean}	Average activity values were determined in intratumoral ROI placed on slice with maximum activity concentration.	2, independent (not mentioned whether blinded)
Chen et al. (*13*)	SUV	Not mentioned.	1, not mentioned whether blinded
Wieder et al. (*14*)	SUV_{mean}	Circular ROIs (1.5 cm in diameter) were manually placed over all tumors at site of maximum ^{18}F-FDG uptake on baseline scan. SUVs normalized to patient body weight were calculated from average activity values in ROI.	Not mentioned
Song et al. (*15*)	SUV_{max}	For semiquantitative analysis of increased ^{18}F-FDG uptake lesion, maximum SUV based on body weight was calculated.	1
Cascini et al. (*16*)	SUV_{mean}	Irregular ROIs were semiautomatically drawn manually on transaxial planes using region-growing method that included pixels above threshold value (between 20% and 50% of maximum pixel value). Table 1: SUV_{mean}.	1, not mentioned whether blinded
Huang et al. (*17*)	SUV_{mean}	ROIs were hand-drawn over tumor for calculation of SUV. ROIs were drawn to follow contours of elevated ^{18}F-FDG activity, as compared with normal tissue, contralateral to tumor site.	Not mentioned
Wieder et al. (*18*)	SUV_{mean}	ROIs were manually placed over each primary tumor. Circular ROI of 1.5 cm (1.5 cm in diameter; 10 pixels) was placed on slice with maximum ^{18}F-FDG uptake. SUVs were calculated using average activity values in ROI.	Not mentioned
Iagaru et al. (*19*)	SUV_{max}	ROIs were placed around regions of increased ^{18}F-FDG uptake for SUV_{max} determination.	Not mentioned
Nishiyama et al. (*20*)	SUV_{max}	SUV was defined as tissue concentration of ^{18}F-FDG (kBq/mL) in structure delineated by ROI divided by activity injected per gram of body weight (kBq/g). ROI was placed over entire primary tumor. SUV_{max} of primary tumor was used.	2, not mentioned whether independent or in consensus or whether blinded
Benz et al. (*21*)	SUV_{max}	Manual delineation of ROI on consecutive axial slices of CT scan was used. SUV_{max} and SUV_{mean} were calculated.	1, blinded
Smithers et al. (*22*)	SUV_{max}	Maximum voxel activity in tumor was used for SUV quantification.	1, not mentioned whether blinded
Ye et al. (*23*)	SUV_{max}	ROIs were individually defined for each patient on transverse sections of PET images. SUV_{max} was measured.	2, independent (blinded)

TBR: tumor-to-background ratio; T/NT: tumor-to-nontumor ratio; DUR: dose uptake ratio; DUR_{BSA} = dose uptake ratio body surface area; SUV_{max} = maximum standardized uptake value; SUV_{mean} = mean standardized uptake value.

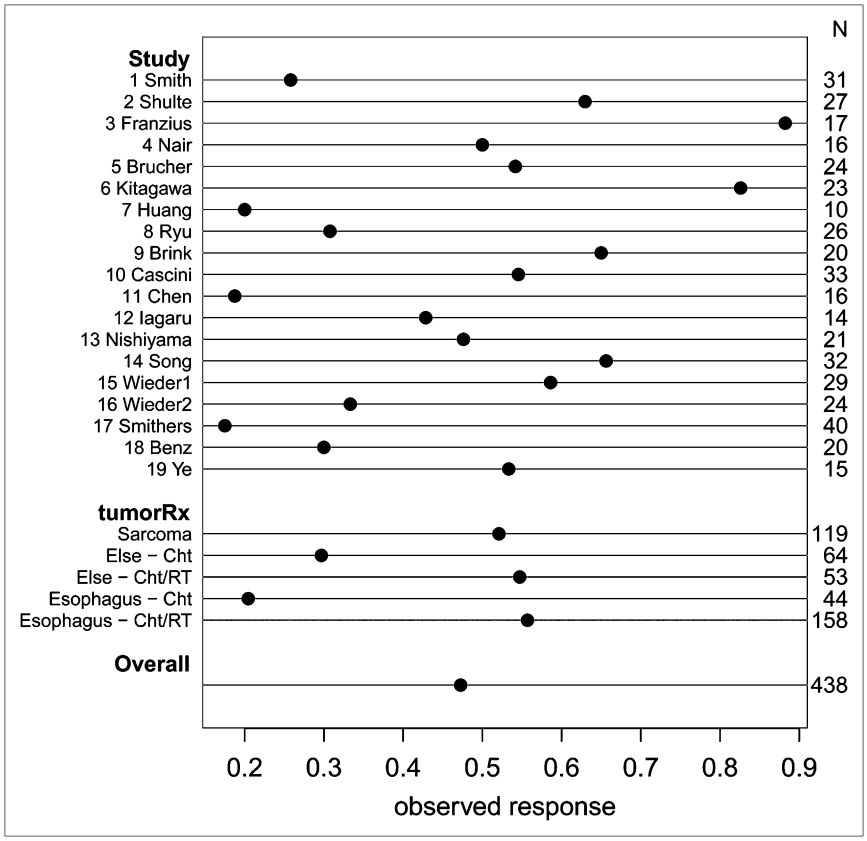

FIGURE 1. Overview of response rates in 19 eligible studies. TumorRx indicates combination of tumor type (sarcoma, esophagus, or other types) and therapy (chemotherapy [ChT] or chemoradiotherapy [ChT/RT]). Sarcoma was exclusively treated by chemoradiotherapy. Tumor-treatment combination mostly explains heterogeneity between studies with respect to factors explaining response.

studies, 6 were on esophageal cancer (46% of patients), 7 on sarcoma (27% of patients), and 6 on other malignancies (breast cancer, head and neck carcinoma, non–small cell lung cancer, gynecologic cancer, and locally advanced rectal cancer; 27% of patients). In 8 studies, each patient received chemotherapy (51% of patients); in the other studies (49% of patients), chemotherapy was combined with radiotherapy in several patients. Radiotherapy was always given concurrently with chemotherapy. Table 1 provides further details of the patient characteristics per study. In all studies, surgical resection of the tumor was scheduled within weeks after completion of the neoadjuvant treatment. The pathologic definition of response differed per malignancy and is displayed in Table 2 (*24–27*). Because studies were performed over a period of almost a decade (1999–2008), no standardized PET protocol was used, and variable scanners, scan modes, ^{18}F-FDG doses, time intervals (between injection of ^{18}F-FDG and the PET scan, between the completion of the induction therapy and the posttreatment PET, and between the posttreatment PET and surgery), and image-reconstruction methods were used. These PET characteristics are listed in Table 3, and in Table 4 the PET data-analysis characteristics are displayed in more detail. Furthermore, the fasting period differed per study. However, all studies reported a fasting period of at least 4 h before PET, except the study of Huang et al., in which this period was at least 2 h (*17*). All but 4 studies (*17,19,20,22*) reported that glucose levels were measured before PET examination. No study, except for the study of Chen et al. (*13*), described when or how the PET or PET/CT scanners were calibrated. Different methods to quantify ^{18}F-FDG uptake were used: the SUV approach was used in 15 studies (maximum standardized uptake value in 7 studies; mean standardized uptake value in 8 studies), tumor-to-background (or nontumor-to-background) ratios in 3 studies, and a dose uptake ratio in 1 study. Different ROI methodologies were used in the analysis (manual; irregular isocontour, based on a fixed percentage of the maximal pixel in the tumor, on a fixed SUV threshold, or on a background-level threshold; or small fixed-dimension ROI centered over the highest-uptake part of the tumor; Table 4).

For all patients, the average overall histopathologic response rate was 0.47 (median, 0.50), ranging from 0.17 to 0.88 among the studies (Fig. 1). Logistic regression estimated the histopathologic response rate as a function of the linear predictor decrease in ^{18}F-FDG uptake, tumor type, and therapy. As illustrated in Figure 2, this model suggests that each 10% relative difference in ^{18}F-FDG uptake corresponded to a 17% positive change in pathologic response rate at the mean level of baseline ^{18}F-FDG uptake (for each tumor-therapy group). Figure 3 illustrates the predicted response according to the multilevel model versus the observed response rate according to histopathology of all 19 studies.

The relative change in ^{18}F-FDG uptake was the strongest indicator ($P < 0.0001$) for predicting histopathologic tumor

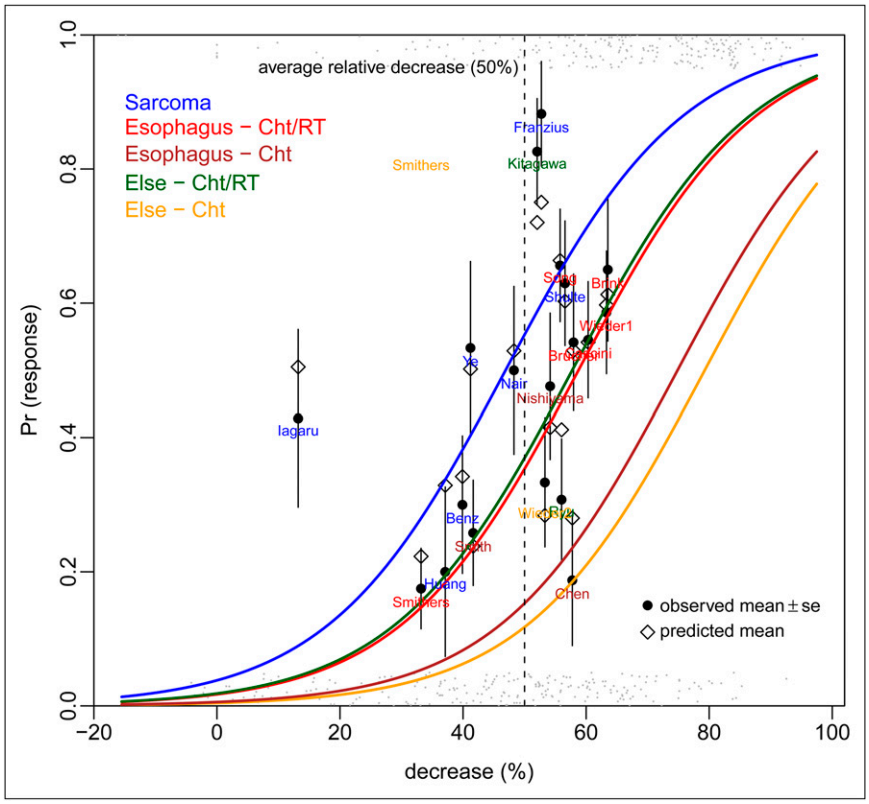

FIGURE 2. Logistic regression estimating histopathologic response rate (Pr [response]) as function of linear predictor of decrease in ^{18}F-FDG uptake (decrease [%]), tumor type, and therapy (indicated by colored lines). Black circles indicate actual average histopathologic response rates per study, whereas open diamonds represent point estimates of response rate. Gray dots at bottom (no response) and top (response) show actual individual patient data. At mean level of baseline (for each tumor-therapy group), model suggests that 10% decrease in relative difference corresponds to 17% increase in pathologic response rate. Cht = chemotherapy; ChT/RT = chemoradiotherapy.

response. Baseline ^{18}F-FDG uptake was not significantly associated as a main factor. However, there was a significant interaction ($P < 0.0001$) between the baseline ^{18}F-FDG uptake and decrease in ^{18}F-FDG uptake. This interaction is illustrated in Figure 4, where 3 quartiles of decrease (25th, 50th, and 75th) are plotted against the baseline ^{18}F-FDG uptake (x-axis) and the probability of histopathologic response (y-axis). Among patients with a high fractional decrease of tracer uptake, those patients with high baseline ^{18}F-FDG uptake values had a higher probability of histopathologic response than did those with low baseline ^{18}F-FDG values. Conversely, among patients with low fractional ^{18}F-FDG reductions, those patients with high baseline ^{18}F-FDG uptake had a lower probability of histopathologic response than did those with low baseline uptake. In the group around the median fractional ^{18}F-FDG decrease, the probability of response was almost constant along the range of baseline ^{18}F-FDG values. Adding the baseline ^{18}F-FDG uptake to the decrease in ^{18}F-FDG uptake significantly improved the prediction ($P < 0.0001$).

Compared with sarcomas (all receiving chemoradiotherapy), esophageal tumors had a lower histopathologic response rate ($P = 0.001$ for chemotherapy and $P = 0.07$ for chemoradiotherapy). This lower histopathologic response rate should be read with the greatly different histopathologic response criteria in mind (Table 2). The response rate of patients with other tumors receiving chemoradiotherapy did not differ from the response rate of sarcomas, but those receiving chemotherapy had the lowest response rate ($P = 0.00063$). Including the type of measurement did not improve the overall fit of the model significantly. Therefore, it was decided to leave the variable out.

The heterogeneity between studies with respect to the factors explaining the response was moderate (MOR, 1.89) and mostly explained by the tumor-treatment combination (interval odds ratio, esophageal chemotherapy, 0.03–0.36; other tumor chemotherapy, 0.04–0.49), also illustrated in Figure 1.

DISCUSSION

This meta-analysis provides evidence to suggest that baseline ^{18}F-FDG uptake adds prognostically relevant information to the relative change of ^{18}F-FDG uptake, in the context of neoadjuvant therapy of extracerebral solid tumors. The overall fit of the model (Fig. 3) suggests that the results are applicable to a broad spectrum of possible response rates and test conditions.

We hypothesized that baseline uptake might add information on responsiveness to relative change because baseline ^{18}F-FDG uptake appears to be related to a more aggressive phenotype, probably mediated via hypoxia or proliferative activity. We also reasoned that the size of such potential effect modification of relative change was unpredictable because proliferation and hypoxia may affect therapy differently: high proliferative activity may be prognostically favorable in the case of chemotherapy, but the reverse may be true for radiotherapy (e.g., via repopulation effects, perhaps as a function of fractionation schemes). Alternatively, hypoxia is supposed to negatively affect the impact of either therapy. Therefore, we chose a phenomenologic rather than mechanistic approach.

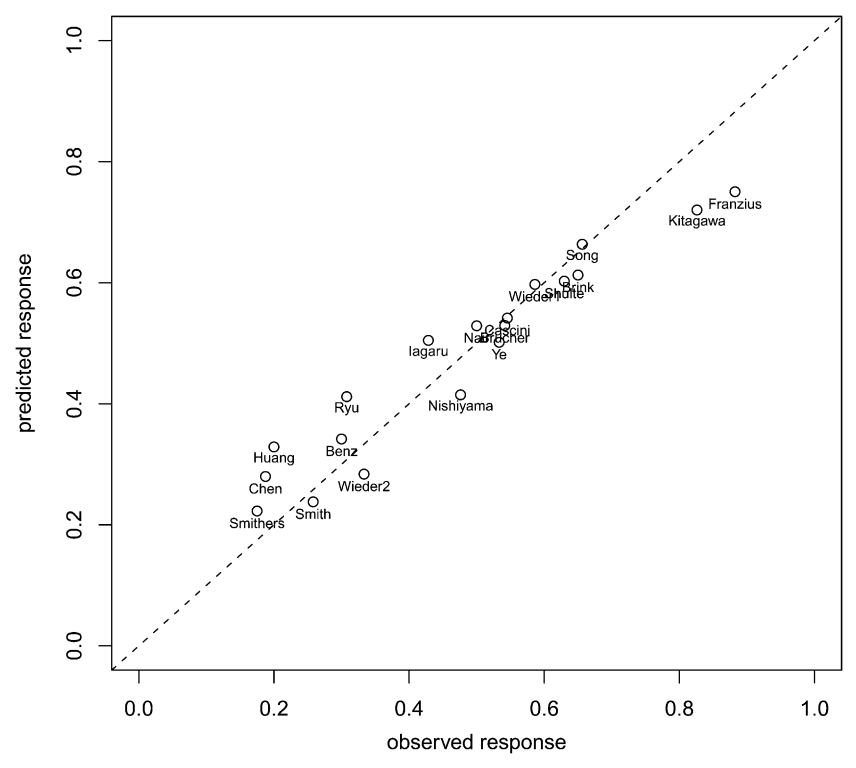

FIGURE 3. Predicted and observed response rate of all 19 studies based on multilevel model with change in ^{18}F-FDG uptake, baseline ^{18}F-FDG uptake, tumor type, and treatment.

Our meta-analytic method accounts for the variability of individual study characteristics. We applied a 2-level model, allowing the variances within and between studies to be different. Simultaneously, several sources of between-study heterogeneity could be considered. Although the heterogeneity between these studies with respect to the factors explaining the response proved to be moderate, each of the separate studies was small and contained a substantial

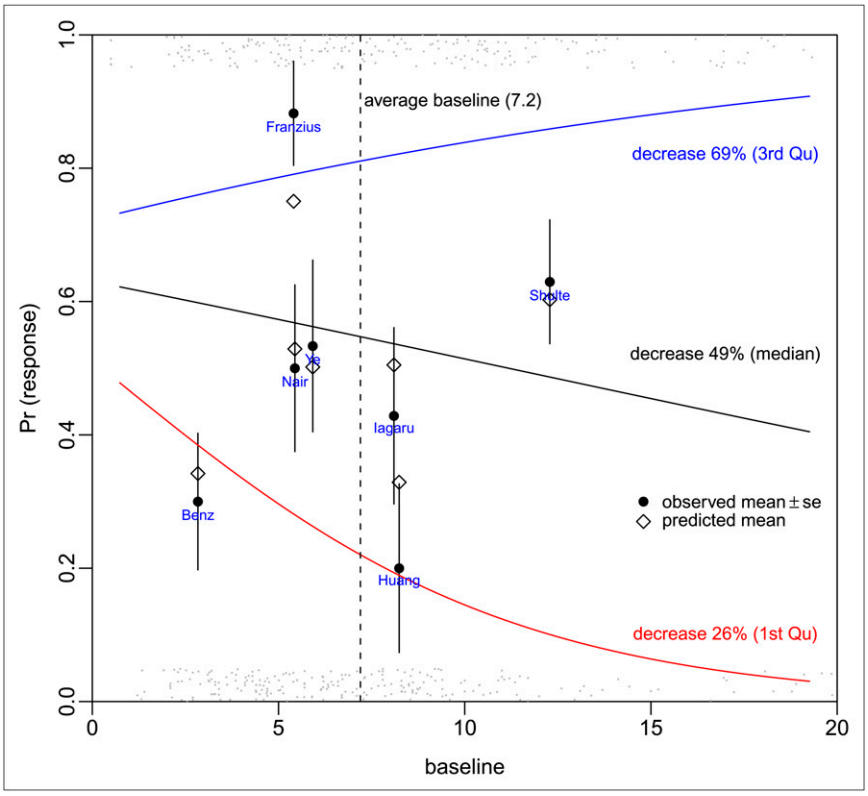

FIGURE 4. Logistic regression estimating response rate (Pr [response]) as function of linear predictor of baseline ^{18}F-FDG uptake at 3 different percentiles of relative decrease (25th, 50th, and 75th percentiles) in ^{18}F-FDG uptake at end of treatment (indicated by colored lines). Black circles indicate actual average response rates, and open diamonds represent point estimates of response rate of studies in sarcoma. Gray dots at bottom (no response) and top (response) show actual individual patient data. Figure clearly shows interaction between level of decrease and baseline ^{18}F-FDG uptake.

heterogeneity in many other aspects. From a quantitative perspective, the findings need to be interpreted with caution: obviously, the model cannot account for technical measurement errors due to low contrast (tumors with low baseline uptake).

Without standardization of, for example, the PET methodology, comparison of results obtained from different centers is hampered by the diversity in methodology of acquisition, image reconstruction, and data-analysis procedures that are applied. To perform multicenter studies, standard protocols should and are being implemented (*28*). The implication of this finding is that standardization of PET methodology in oncologic trials should be intensified: to aggregate the evidence, it becomes even more important to standardize PET methodology, because the use of absolute values imposes stronger methodologic rigor than that of relative change alone. Obviously, an analysis of a study population with 1 type of tumor, treatment, and timing of scans relative to treatment improves homogeneity even further.

Additionally, this meta-analysis would have had more power if the community had adopted the habit of at least electronically publishing the individual patient results as a standard approach. It may be assumed that it is not feasible to report individual data in larger studies.

In this meta-analysis, we focused on chemotherapy as the mode of systemic therapy. Whether these findings can be extrapolated to newer forms of targeted therapy is unclear, because the interaction of ^{18}F-FDG metabolism and therapy does not need to be consistent.

CONCLUSION

This meta-analysis supports the hypothesis of an interaction of baseline ^{18}F-FDG uptake with its relative change during therapy in patients treated with neoadjuvant chemoradiotherapy. These data corroborate and extend the need for standardization, quality assurance, and control of PET studies quantifying ^{18}F-FDG in oncologic treatment monitoring. Obviously, such standardization will also allow proper validation of the current findings.

ACKNOWLEDGMENTS

We thank Tim van den Wijngaert, University of Antwerp, Antwerp, Belgium, for his contribution to this study.

REFERENCES

1. Fletcher JW, Djulbegovic B, Soares HP, et al. Recommendations on the use of ^{18}F-FDG PET in oncology. *J Nucl Med.* 2008;49:480–508.
2. Berghmans T, Dusart M, Paesmans M, et al. Primary tumor standardized uptake value (SUVmax) measured on fluorodeoxyglucose positron emission tomography (FDG-PET) is of prognostic value for survival in non-small cell lung cancer (NSCLC): a systematic review and meta-analysis (MA) by the European Lung Cancer Working Party for the IASLC Lung Cancer Staging Project. *J Thorac Oncol.* 2008;3:6–12.
3. Harrell FE Jr. *Regression Modeling Strategies: With Applications To Linear Models, Logistic Regression and Survival Analysis.* New York: Springer; 2001.
4. Larsen K, Merlo J. Appropriate assessment of neighborhood effects on individual health: integrating random and fixed effects in multilevel logistic regression. *Am J Epidemiol.* 2005;161:81–88.
5. Schulte M, Brecht-Krauss D, Werner M, et al. Evaluation of neoadjuvant therapy response of osteogenic sarcoma using FDG PET. *J Nucl Med.* 1999;40:1637–1643.
6. Franzius C, Sciuk J, Brinkschmidt C, Jurgens H, Schober O. Evaluation of chemotherapy response in primary bone tumors with F-18 FDG positron emission tomography compared with histologically assessed tumor necrosis. *Clin Nucl Med.* 2000;25:874–881.
7. Smith IC, Welch AE, Hutcheon AW, et al. Positron emission tomography using [^{18}F]-fluorodeoxy-D-glucose to predict the pathologic response of breast cancer to primary chemotherapy. *J Clin Oncol.* 2000;18:1676–1688.
8. Nair N, Ali A, Green AA, et al. Response of osteosarcoma to chemotherapy. evaluation with F-18 FDG-PET scans. *Clin Positron Imaging.* 2000;3:79–83.
9. Brücher BL, Weber W, Bauer M, et al. Neoadjuvant therapy of esophageal squamous cell carcinoma: response evaluation by positron emission tomography. *Ann Surg.* 2001;233:300–309.
10. Ryu JS, Choi NC, Fischman AJ, Lynch TJ, Mathisen DJ. FDG-PET in staging and restaging non-small cell lung cancer after neoadjuvant chemoradiotherapy: correlation with histopathology. *Lung Cancer.* 2002;35:179–187.
11. Kitagawa Y, Nishizawa S, Sano K, et al. Prospective comparison of ^{18}F-FDG PET with conventional imaging modalities (MRI, CT, and ^{67}Ga scintigraphy) in assessment of combined intraarterial chemotherapy and radiotherapy for head and neck carcinoma. *J Nucl Med.* 2003;44:198–206.
12. Brink I, Hentschel M, Bley TA, et al. Effects of neoadjuvant radiochemotherapy on ^{18}F-FDG-PET in esophageal carcinoma. *Eur J Surg Oncol.* 2004;30:544–550.
13. Chen X, Moore MO, Lehman CD, et al. Combined use of MRI and PET to monitor response and assess residual disease for locally advanced breast cancer treated with neoadjuvant chemotherapy. *Acad Radiol.* 2004;11:1115–1124.
14. Wieder HA, Brucher BL, Zimmermann F, et al. Time course of tumor metabolic activity during chemoradiotherapy of esophageal squamous cell carcinoma and response to treatment. *J Clin Oncol.* 2004;22:900–908.
15. Song SY, Kim JH, Ryu JS, et al. FDG-PET in the prediction of pathologic response after neoadjuvant chemoradiotherapy in locally advanced, resectable esophageal cancer. *Int J Radiat Oncol Biol Phys.* 2005;63:1053–1059.
16. Cascini GL, Avallone A, Delrio P, et al. ^{18}F-FDG PET is an early predictor of pathologic tumor response to preoperative radiochemotherapy in locally advanced rectal cancer. *J Nucl Med.* 2006;47:1241–1248.
17. Huang TL, Liu RS, Chen TH, Chen WY, Hsu HC, Hsu YC. Comparison between F-18-FDG positron emission tomography and histology for the assessment of tumor necrosis rates in primary osteosarcoma. *J Chin Med Assoc.* 2006;69:372–376.
18. Wieder HA, Ott K, Lordick F, et al. Prediction of tumor response by FDG-PET: comparison of the accuracy of single and sequential studies in patients with adenocarcinomas of the esophagogastric junction. *Eur J Nucl Med Mol Imaging.* 2007;34:1925–1932.
19. Iagaru A, Masamed R, Chawla SP, Menendez LR, Fedenko A, Conti PS. F-18 FDG PET and PET/CT evaluation of response to chemotherapy in bone and soft tissue sarcomas. *Clin Nucl Med.* 2008;33:8–13.
20. Nishiyama Y, Yamamoto Y, Kanenishi K, et al. Monitoring the neoadjuvant therapy response in gynecological cancer patients using FDG PET. *Eur J Nucl Med Mol Imaging.* 2008;35:287–295.
21. Benz MR, len-Auerbach MS, Eilber FC, et al. Combined assessment of metabolic and volumetric changes for assessment of tumor response in patients with soft-tissue sarcomas. *J Nucl Med.* 2008;49:1579–1584.
22. Smithers BM, Couper GC, Thomas JM, et al. Positron emission tomography and pathological evidence of response to neoadjuvant therapy in adenocarcinoma of the esophagus. *Dis Esophagus.* 2008;21:151–158.
23. Ye Z, Zhu J, Tian M, et al. Response of osteogenic sarcoma to neoadjuvant therapy: evaluated by ^{18}F-FDG-PET. *Ann Nucl Med.* 2008;22:475–480.
24. Mandard AM, Dalibard F, Mandard JC, et al. Pathologic assessment of tumor regression after preoperative chemoradiotherapy of esophageal carcinoma. Clinicopathologic correlations. *Cancer.* 1994;73:2680–2686.
25. Salzer-Kuntschik M, Delling G, Beron G, Sigmund R. Morphological grades of regression in osteosarcoma after polychemotherapy - study COSS 80. *J Cancer Res Clin Oncol.* 1983;106(suppl):21–24.
26. Sharkey FE, Addington SL, Fowler LJ, et al. Effects of preoperative chemotherapy on the morphology of resectable breast carcinoma. *Mod Pathol.* 1996;9:893–900.
27. Aktepe F, Kapucuolgu N, Pak I. The effects of chemotherapy on breast cancer tissue in locally advanced breast cancer. *Histopathology.* 1996;29:63–67.
28. Boellaard R, Oyen WJ, Hoekstra CJ, et al. The Netherlands protocol for standardisation and quantification of FDG whole body PET studies in multicentre trials. *Eur J Nucl Med Mol Imaging.* 2008;35:2320–2333.
29. Schmidlin P. Improved iterative image reconstruction using variable projection binning and abbreviated convolution. *Eur J Nucl Med.* 1994;21:930–936.